Probing the Efficiency of Electron Transfer through Porphyrin-Based Molecular Wires

Mikael U. Winters,[†] Emma Dahlstedt,[‡] Holly E. Blades,[‡] Craig J. Wilson,[‡]
Michael J. Frampton,[‡] Harry L. Anderson,*,[‡] and Bo Albinsson*,[†]

Contribution from the Department of Chemical and Biological Engineering, Physical Chemistry, Kemivägen 3, SE - 412 96 Göteborg, Sweden, and the Department of Chemistry, University of Oxford, Chemistry Research Laboratory, Mansfield Road, Oxford OX1 3TA, United Kingdom

Received October 18, 2006; E-mail: balb@chalmers.se; harry.anderson@chem.ox.ac.uk

Abstract: Electron transfer over long distances is important for many future applications in molecular electronics and solar energy harvesting. In these contexts, it is of great interest to find molecular systems that are able to efficiently mediate electrons in a controlled manner over nanometer distances, that is, structures that function as molecular wires. Here we investigate a series of butadiyne-linked porphyrin oligomers with ferrocene and fullerene (C_{60}) terminals separated by one, two, or four porphyrin units ($\mathbf{P_n}$, $n = 1$, 2, or 4). When the porphyrin oligomer bridges are photoexcited, long-range charge separated states are formed through a series of electron-transfer steps and the rates of photoinduced charge separation and charge recombination in these systems were elucidated using time-resolved absorption and emission measurements. The rates of long-range charge recombination, through these conjugated porphyrin oligomers, are remarkably fast ($k_{CR2} = 15 - 1.3 \times 10^8$ s^{-1}) and exhibit very weak distance dependence, particularly comparing the systems with $n = 2$ and $n = 4$. The observation that the porphyrin tetramer mediates fast long-range charge transfer, over 65 Å, is significant for the application of these structures as molecular wires.

Introduction

The rate of electron transfer between molecules is a sensitive function not only of parameters relating to the electron donor and acceptor but also of the medium connecting them. The driving force ($\Delta G°$) and reorganization energy (λ) are such donor and acceptor parameters, while the electronic coupling (V) is governed by the bridging structure as well as by the donor–bridge energy gap.[1] Many different molecular bridges have been studied,[2–9] and the rate of electron transfer as a function of donor–acceptor separation (R) is often described by the exponential expression in eq 1.

$$k = k_0 e^{-\beta R} \tag{1}$$

The ability of the bridge to mediate electron transfer is quantified by the attenuation factor β, which varies with the degree of conjugation in the bridge and also with the donor–bridge energy gap (i.e., the height of the tunneling barrier). In theory, values of β should range from 0 for a metallic bridge to 3–5 Å^{-1} for electron transfer through a vacuum.[9] Most organic π-conjugated bridges give attenuation factors in the range 0.2–0.6 Å^{-1},[2–5] but recently several systems have been reported with extraordinarily lower values ($\beta = 0.01$–0.06 Å^{-1}),[7,8] which could open up the possibility of using molecular wires for taking charge over longer distances.

Conjugated porphyrin oligomers feature long strongly coupled π-systems and small π–π^* gaps, so they are expected to be good mediators for long-range electron transfer.[10,11] For example Osuka and co-workers have shown that edge-fused porphyrin oligomers with lengths of up to 70 Å conduct charge efficiently across break-junctions.[12] Recently Therien et al. have reported

[†] Chalmers University of Technology.
[‡] University of Oxford.

(1) Eng, M. P.; Albinsson, B. *Angew. Chem., Int. Ed.* **2006**, *45*, 5626−5629.
(2) Helms, A.; Heiler, D.; McLendon, G. *J. Am. Chem. Soc.* **1992**, *114*, 6227−6238.
(3) Sachs, S. B.; Dudek, S. P.; Hsung, R. P.; Sita, L. R.; Smalley, J. F.; Newton, M. D.; Feldberg, S. W.; Chidsey, C. E. D. *J. Am. Chem. Soc.* **1997**, *119*, 10563−10564.
(4) (a) Creager, S.; Yu, C. J.; Bamdad, C.; O'Connor, S.; MacLean, T.; Lam, E.; Chong, Y.; Olsen, G. T.; Luo, J.; Gozin, M.; Kayyem, J. F. *J. Am. Chem. Soc.* **1999**, *121*, 1059−1064. (b) Wiberg, J.; Guo, L.; Pettersson, K.; Nilsson, D.; Ljungdahl, T.; Mårtensson, J.; Albinsson, B, *J. Am. Chem. Soc.* **2007**, *129*, 155−163.
(5) Pettersson, K.; Wiberg, J.; Ljungdahl, T.; Mårtensson, J.; Albinsson, B. *J. Phys. Chem. A* **2006**, *110*, 319−326. Eng, M. P.; Ljungdahl, T.; Mårtensson, J.; Albinsson, B. *J. Phys. Chem. B* **2006**, *110*, 6483−6491.
(6) Imahori, H.; Tamaki, K.; Guldi, D. M.; Luo, C.; Fujitsuka, M.; Ito, O.; Sakata, Y.; Fukuzumi, S. *J. Am. Chem. Soc.* **2001**, *123*, 2607−2617. Guldi, D. M.; Imahori, H.; Tamaki, K.; Kashiwagi, Y.; Yamada, H.; Sakata, Y.; Fukuzumi, S. *J. Phys. Chem. A* **2004**, *108*, 541−548.
(7) Giacalone, F.; Segura, J. L.; Martín, N.; Ramey, J.; Guldi, D. M. *Chem. Eur. J.* **2005**, *11*, 4819−4834. de la Torre, G.; Giacalone, F.; Segura, J. L.; Martín, N.; Guldi, D. M. *Chem.−Eur. J.* **2005**, *11*, 1267−1280.

(8) Vail, S. A.; Krawczuk, P. J.; Guldi, D. M.; Palkar, A.; Echegoyen, L.; Tomé, J. P. C.; Fazio, M. A.; Schuster, D. I. *Chem.−Eur. J.* **2005**, *11*, 3375−3388.
(9) Gray, H. B.; Winkler, J. R. *Proc. Natl. Acad. Sci. U.S.A.* **2005**, *102*, 3534. Paddon-Row, M. N. In *Electron Transfer in Chemistry*; Balzani, V., Ed.; Wiley-VCH, Weinheim, 2001; Vol. 3, pp 201−215.
(10) Anderson, H. L. *Chem. Commun.* **1999**, 2323−2330.
(11) Kim, D.; Osuka, A. *Acc. Chem. Res.* **2004**, *37*, 735−745.
(12) Yoon, D. H.; Lee, S. B.; Yoo, K.-H.; Kim, J.; Lim, J. K.; Aratani, N.; Tsuda, A.; Osuka, A.; Kim, D. *J. Am. Chem. Soc.* **2003**, *125*, 11062−11064. Kang, B. K.; Aratani, N.; Lim, J. K.; Kim, D.; Osuka, A.; Yoo, K.-H. *Chem. Phys. Lett.* **2005**, *412*, 303−306.
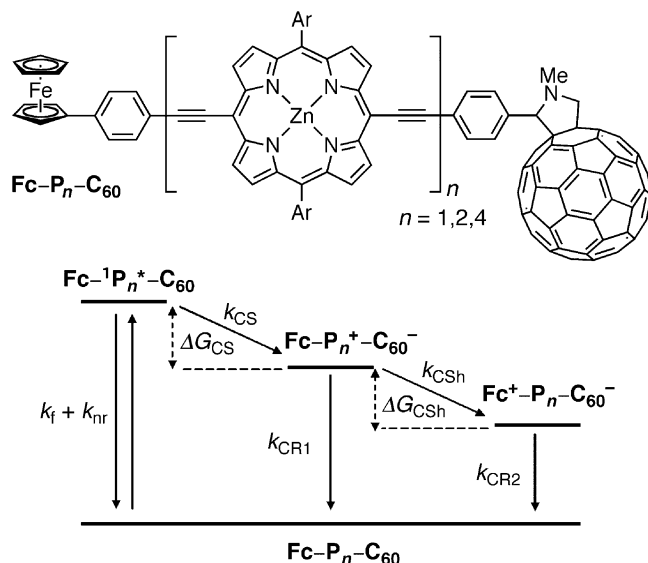
Figure 1. General structure of the triads and schematic energy level diagram showing the charge separation (CS), charge shift (CSh), and charge recombination (CR1 and CR2) reactions. (The aryl substituents, Ar, are 3,5-di(*tert*-butyl)phenyl for $n = 1$ and 3,5-di(octyloxy)phenyl for $n = 2$ and 4.)

EPR measurements indicating that ethyne-linked porphyrin oligomers can mediate essentially barrierless hole transport over distances of up to 75 Å.[13] In this study we have tested the efficiency of electron transfer through porphyrin-based molecular wires by measuring the rate of charge recombination in a series of donor–bridge–acceptor molecules, $Fc^+-P_n-C_{60}^-$, in which the electron donor (C_{60}^-) is connected to the electron acceptor (Fc^+) via a set of butadiyne-linked porphyrin oligomers (P_n, $n = 1$, 2, or 4). Surprisingly, the rate of electron transfer through the porphyrin tetramer bridge (P_4, length 65 Å) is almost the same as that through the dimer (P_2, length 38 Å); just comparing these two bridges gives an apparent attenuation factor of $\beta = 0.003$ Å^{-1}. Many ferrocene–porphyrin–fullerene triads have been investigated previously by Fukuzumi and co-workers,[6] with the aim of preparing long-lived charge separated states. The aim of this study is completely different: we are not primarily interested in the lifetimes of the charge separated states but rather to investigate whether the intervening bridge acts as an efficient molecular wire.

Electron-transfer reactions can be very fast, and thus it is often beneficial to study photoinduced electron transfer in which either the donor or acceptor is excited to prepare an initial state with a driving force for electron transfer. Our conjugated porphyrin oligomers have very low-lying singlet excited states,[14] so it is difficult to find a donor or acceptor that could be excited without transferring energy to the bridge. Therefore a slightly different design was chosen, in which the porphyrin oligomers were appended with a primary electron acceptor (C_{60}) and a secondary electron donor (ferrocene, Fc). Figure 1 shows the anticipated processes that occur in the triads $Fc-P_n-C_{60}$, after excitation of the porphyrin oligomer. Initially, a primary charge separation involving the transfer of an electron from the excited porphyrin oligomer to C_{60} occurs. This is followed by a charge shift

(13) Susumu, K.; Frail, P. R.; Angiolillo, P. J.; Therien, M. J. *J. Am. Chem. Soc.* **2006**, *128*, 8380–8381.
(14) Taylor, P. N.; Huuskonen, J.; Rumbles, G.; Aplin, R. T.; Williams, E.; Anderson, H. L. *Chem. Commun.* **1998**, 909–910.

involving the ferrocene moiety as a secondary donor that repopulates the hole on the porphyrin oligomer and, thus, recreates the bridge in the ground state. The fully charge separated state, $Fc^+-P_n-C_{60}^-$, recombines to the ground state with a rate constant k_{CR2}. In this recombination process the electron transfer occurs from C_{60}^- (which now acts as a donor) to Fc^+ (now the acceptor) and the electronic coupling is mediated by the porphyrin oligomer in its electronic ground state. The purpose of this study is to relate the magnitude of k_{CR2} to the length and electronic structure of the porphyrin oligomer bridges. Ferrocene and C_{60} were chosen as the donor and acceptor because their redox potentials make both the charge-separation and charge-shift steps in Figure 1 thermodynamically favorable for any length of porphyrin oligomer bridge.

Results and Discussion

Synthesis. The triads $Fc-P_n-C_{60}$, the silicon terminated reference dyads $Fc-P_n-Si$, and $Si-P_n-C_{60}$, and reference 4-butylphenyl-terminated bridges $Bu-P_n-Bu$ were all synthesized ($n = 1$, 2, and 4) from the silicon-terminated oligomers $Si-P_n-Si$ using Sonogashira coupling methodology, as shown in Scheme 1 (see Supporting Information for yields, experimental details, and characterization data). The triads $Fc-P_n-C_{60}$ were synthesized via both routes A and B; in general route B is more convenient because the presence of the aldehyde substituent in $Si-P_n-CHO$ facilitates its chromatographic purification, compared with $Fc-P_n-Si$.

Absorption Spectra, Emission Spectra, and Electrochemistry. The absorption and emission spectra of these porphyrin oligomers show a progressive shift to longer wavelengths with increasing oligomer length, as discussed previously.[10,14] The ferrocene and fullerene substituents show little ground state interaction with the porphyrin oligomer bridges, and the absorption spectra of the $Fc-P_n-C_{60}$ triads are essentially superimposable with those of the corresponding $Bu-P_n-Bu$ reference compounds (see Supporting Information). In addition to characterizing the ground state absorption and emission spectra of these $Fc-P_n-C_{60}$ triads and reference systems, the spectra of the transient species involved in the electron-transfer steps were recorded after electrochemical generation. These spectra are important for identification of charge-separated species in transient absorption experiments. In the Supporting Information, spectra of the radical cations of the appropriately substituted porphyrin oligomer references, radical anion of C_{60}, and the radical cation of ferrocene are shown. The intensities and band maxima of the lowest transition in $Si-P_n^+-Si$ are strongly dependent on the size of the oligomers. $Si-P_1^+-Si$ shows distinct peaks at 630 and 716 nm and minor peaks at 800 and 900 nm, whereas $Si-P_2^+-Si$ exhibits an intense band at 964 nm, and $Si-P_4^+-Si$, at 1010 nm.[15] The radical anion, C_{60}^-, shows moderately strong bands at 920 and 1070 nm in the near IR, and the ferrocene radical cation, a weak band at 750 nm. The electrochemistry of these species was investigated in detail, so that we can determine the energies of the charge transfer states. For example the cyclic and square wave voltammograms of the $Bu-P_n-Bu$ bridges in Figure 2 show that the first oxidation and reduction waves are split progressively in the dimer and tetramer. The voltammograms of $Fc-$

(15) Arnold, D. P.; Hartnell, R. D.; Heath, G. A.; Newby, L.; Webster, R. D. *Chem. Commun.* **2002**, 754–755.

Scheme 1 [a]
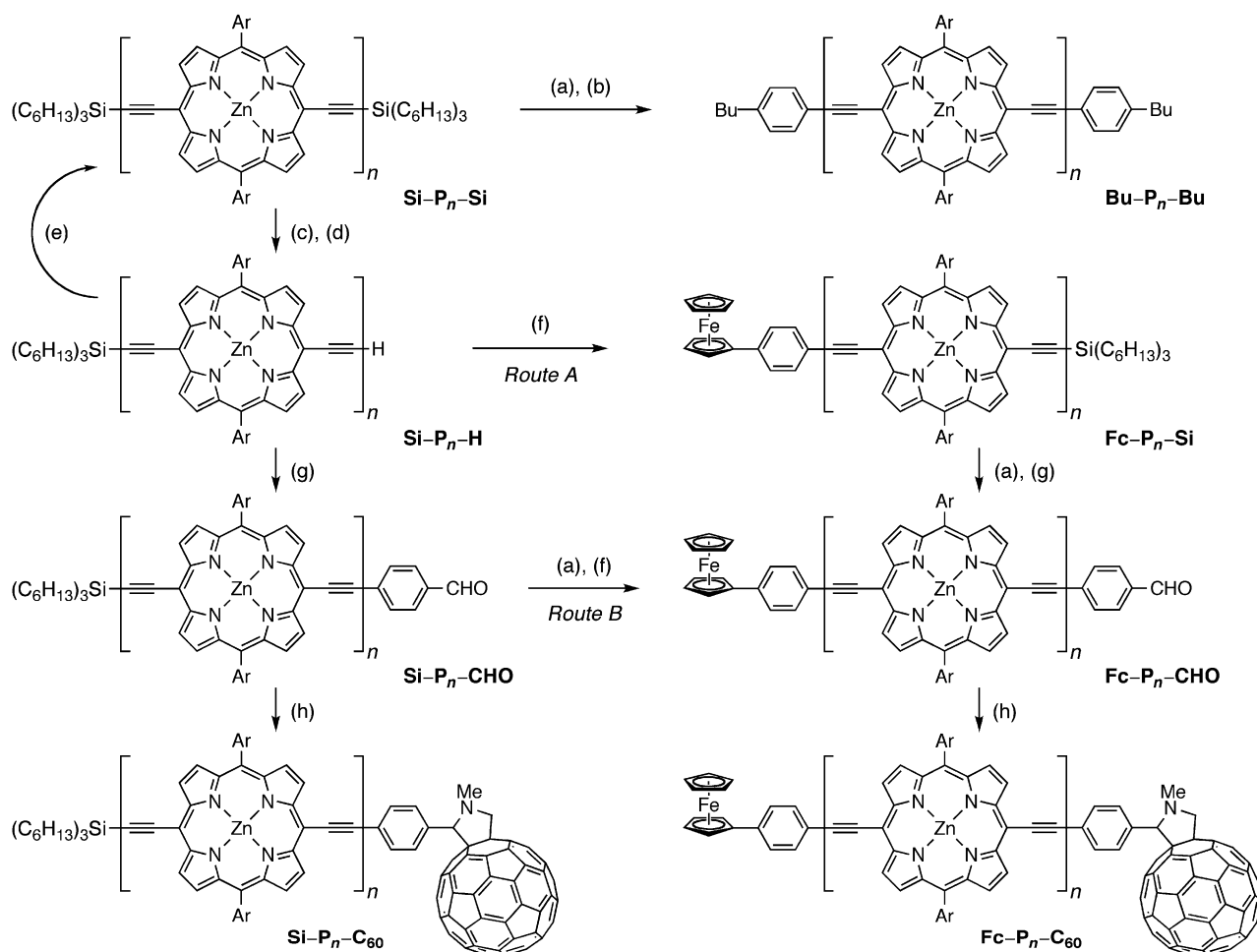
[a] (a) TBAF, CH₂Cl₂; (b) BuC₆H₄I, Pd₂(dba)₃, CuI, PPh₃, NEt₃, PhMe, 40 °C; (c) TBAF, 1:1 CH₂Cl₂, CHCl₃; (d) separation; (e) CuCl, TMEDA, CH₂Cl₂, O₂ ($n \rightarrow 2n$); (f) FcC₆H₄I, Pd₂(dba)₃, CuI, PPh₃, NEt₃, PhMe, 40 °C; (g) IC₆H₄CHO, Pd₂(dba)₃, CuI, PPh₃, NEt₃, PhMe, 40 °C; (h) C₆₀, CH₃NHCH₂CO₂H, PhMe, reflux.

P_1–C_{60} illustrated in Figure 3 show that the Fc/Fc^+ and $C_{60}/$ C_{60}^- redox waves are readily identified; these redox potentials do not change as the length of the intervening porphyrin bridge is increased. The energies of the triplet states of the bridges Bu–$^3P_n^*$–Bu were estimated from low-temperature phosphorescence measurements and agree well with calculated values (Supporting Information). These experiments enabled us to estimate the energies of the states plotted in Figure 4.

Time-Resolved Photophysical Measurements. The charge separation processes in the Fc–P_n–C_{60} triads were followed by femtosecond transient absorption and time-resolved fluorescence. The cascade of electron-transfer reactions leading to the fully charge separated state is moderately complex, and therefore the components Si–P_n–Si, Si–P_n–C_{60}, and Fc–P_n–Si were also investigated. All measurements were fitted to sums of exponential decay functions, and the first-order rate constants were extracted with reference to the model in Figure 1. In Table 1, the decay lifetimes for the triads, dyads, and oligomers are collected, while Table 2 comprises the extracted rate constants, quantum yields, and driving forces for the different processes. The fluorescence from $^1P_n^*$ is almost completely quenched when the fullerene acceptor is attached and the lifetime of the singlet excited state, as judged from transient absorption (Si–P_1–C_{60}, Si–P_2–C_{60}, and Si–P_4–C_{60}) or time-resolved fluorescence (Si–P_4–C_{60}), is significantly reduced compared to Si–

P_n–Si. In the moderately polar solvent used (THF), there was no sign of the formation of C_{60}^*, whereas the anticipated radical ion pairs were readily detected, showing that charge separation is very efficient in the Si–P_n–C_{60} dyads and, indeed, the estimated quantum yields for charge separation approach 100%. In Figure 5, the transient absorption of the P_n–C_{60} systems probed at 1000 nm are displayed, and it is evident that the rise times, as well as the decay times, are becoming progressively longer as n increases. The rate of the initial charge separation, k_{CS}, is calculated from eq 2:

$$k_{CS} = 1/\tau_{21} - 1/\tau_{11} \qquad (2)$$

where τ_{21} and τ_{11} are the lifetimes of the lowest porphyrin singlet excited state of Si–P_n–C_{60} and Si–P_n–Si, respectively (Table 1). A tentative analysis using the Marcus equation[16] showed that the extracted rates are consistent with a reorganization energy between 0.49 and 0.64 eV for $n = 1$–4.[17] This agrees well with the typically low values found for porphyrin–fullerene couples, as well as with estimates obtained from the Born

(16) It does not significantly benefit the analysis to introduce more advanced treatments, such as that of Jortner and co-workers: Ulstrup, J.; Jortner, J. *J. Chem. Phys.* **1975**, *63*, 4358–4368. Jortner, J; Bixon, M. J. *J. Chem. Phys.* **1988**, *88*, 167–170.
(17) Marcus, R. A.; Sutin, N. *Biochim. Biophys. Acta* **1985**, *811*, 265–322. Marcus, R. A. *J. Chem. Phys.* **1956**, *24*, 966–978.
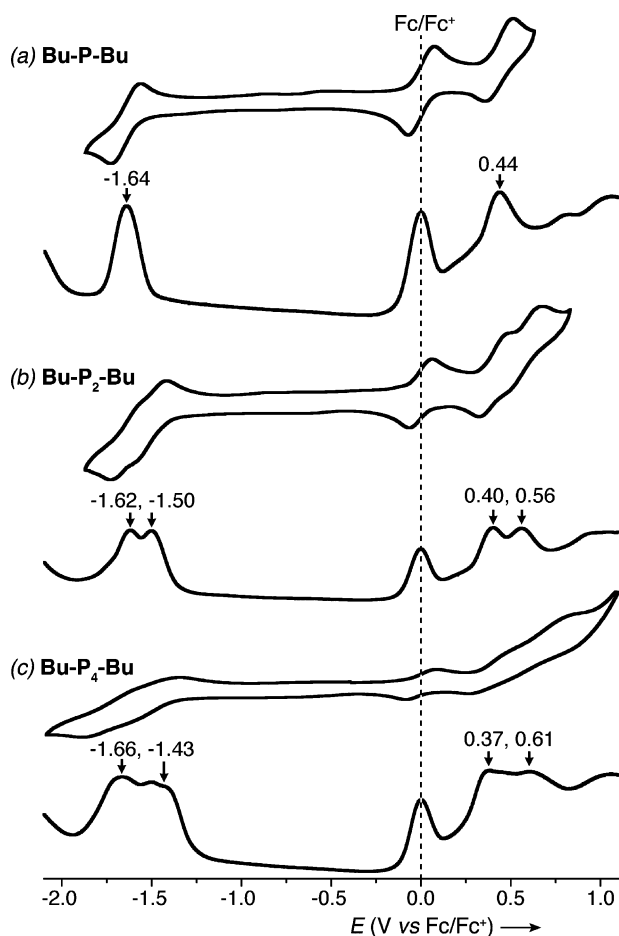
Figure 2. Cyclic and square-wave voltammograms of reference porphyrin oligomers **Bu−P−Bu** monomer (a), **Bu−P₂−Bu** dimer (b), and **Bu−P₄−Bu** tetramer (c), all in THF containing Bu_4NBF_4 (0.1 M), referenced to internal ferrocene (Fc/Fc⁺). Arrows indicate the redox potentials for the first reduction and oxidation of **Bu−P−Bu**, the first and second reductions and oxidations of **Bu−P₂−Bu**, and the first and third/fourth reductions and oxidations of **Bu−P₄−Bu**. Cyclic voltammetry: scan rate 0.25 V s⁻¹; square wave voltammetry: step potential 2 mV, step amplitude 20 mV, square wave frequency 8 Hz; glassy carbon working electrode, Pt counter electrode, $Ag/AgNO_3$ reference electrode.

dielectric continuum model.[18] For the sake of this analysis, the porphyrin−fullerene electronic coupling was assumed to be approximately the same for all $\mathbf{Si-P_n-C_{60}}$, $V = 22.5 \pm 3$ cm⁻¹.

When the corresponding measurements were made on the triads ($\mathbf{Fc-P_n-C_{60}}$), even larger quenching of the singlet excited-state lifetimes were observed (cf. Table 1). Although surprising at first, the explanation was simply that the presence of ferrocene also quenched the porphyrin excited state by a parallel process. Measurements on the dyads, $\mathbf{Fc-P_n-Si}$, gave the rate constants for the ferrocene quenching, k_Q. Having this information the rate constants for the initial charge separation in the triads could also be calculated from eq 3:

$$k_{CS} = 1/\tau_{31} - 1/\tau_{11} - k_Q \qquad (3)$$

where τ_{31} is the singlet excited-state lifetimes of the porphyrin oligomers in $\mathbf{Fc-P_n-C_{60}}$. As expected, the rate for initial charge separation is similar in the dyads and triads, but the corresponding quantum yield (Table 2) is significantly lower in the triads
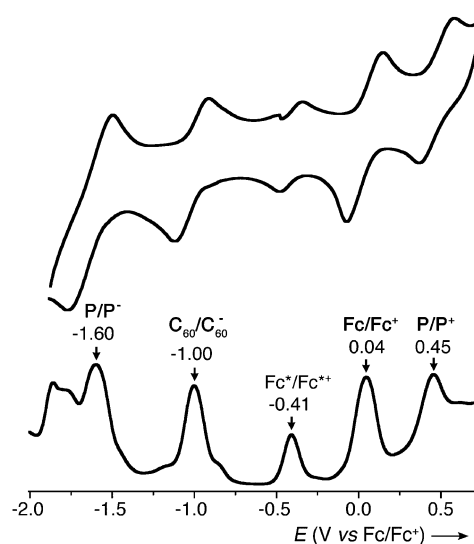
(18) Marcus, R. A. *Can. J. Chem.* **1959**, *37*, 155−163. Marcus, R. A. *J. Chem. Phys.* **1965**, *43*, 679−701.

Figure 3. Cyclic and square-wave voltammograms of monomer triad $\mathbf{Fc-P-C_{60}}$ in THF containing Bu_4NBF_4 (0.1 M). Potentials are given relative to ferrocene (Fc/Fc⁺) but referenced to internal decamethylferrocene (Fc*/Fc*⁺). Scan parameters same as those for Figure 2.
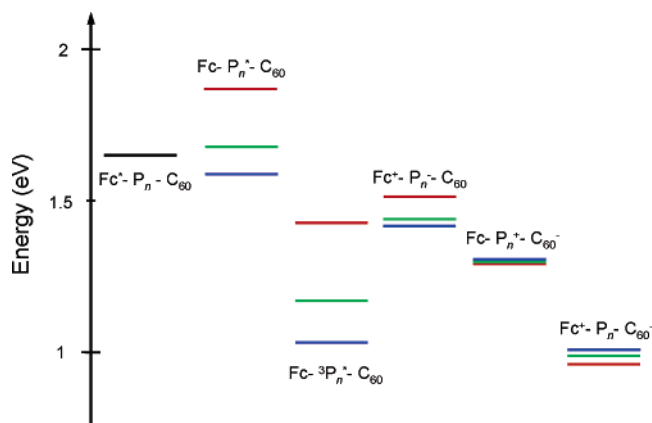

Figure 4. State energies estimated from electrochemical and spectroscopic data (Supporting Information). Red lines are for $n = 1$; green lines, for $n = 2$; and blue lines, for $n = 4$.

Table 1. Lifetimes Extracted from Global Fitting of Transient Absorption Data to Sums of Exponential Decay Functions[a]

	lifetime	monomer $n = 1$	dimer $n = 2$	tetramer $n = 4$
Si−Pₙ−Si	τ_{11} (ps)	1450[b]	1260[b]	830[b]
Si−Pₙ−C₆₀	τ_{21} (ps)	6.1	7.2	29[b]
	τ_{22} (ps)	130	157	293
Fc−Pₙ−C₆₀	τ_{31} (ps)	2.7	5.9	18
	τ_{32} (ps)	30	41	175
	τ_{33} (ps)	640	7100	7800

[a] Four to six different wavelengths, chosen at relevant peaks in the spectra, were used for global analysis of transient absorption data. Errors in the lifetimes are 10% or less. [b] Also from time-resolved fluorescence.

(37−81%) due to the competing quenching by ferrocene. We have not investigated the ferrocene quenching in any detail. However, no new absorption features were formed and no long-lived transient species ($\tau > 100$ ps) could be observed in measurements on $\mathbf{Fc-P_n-Si}$, which suggests that the fluorescence quenching in $\mathbf{Fc-P_n-Si}$ is caused by energy transfer to low lying ferrocene excited states[18] followed by rapid deactivation.

Table 2. First-Order Rate Constants (k) and Driving Forces ($\Delta G°$) as Defined by Figure 1 and Quantum Yields (Φ) for the Charge-Transfer Reactions

process	$\Delta G°[eV]^a$	k	$\Phi[\%]^{b,c}$
$\mathbf{Fc-P^*-C_{60} \rightarrow Fc-P^+-C_{60}^-}$	-0.58	$(6.1\ ps)^{-1}$	37^b
$\mathbf{Fc-P^+-C_{60}^- \rightarrow Fc^+-P-C_{60}^-}$	-0.33	$(39\ ps)^{-1}$	29^c
$\mathbf{Fc-P^+-C_{60}^- \rightarrow Fc-P-C_{60}}$	-1.29	$(130\ ps)^{-1}$	
$\mathbf{Fc^+-P-C_{60}^- \rightarrow Fc-P-C_{60}}$	-0.96	$(640\ ps)^{-1}$	
$\mathbf{Fc-P_2^*-C_{60} \rightarrow Fc-P_2^+-C_{60}^-}$	-0.38	$(7.2\ ps)^{-1}$	81^b
$\mathbf{Fc-P_2^+-C_{60}^- \rightarrow Fc^+-P_2-C_{60}^-}$	-0.31	$(55\ ps)^{-1}$	61^c
$\mathbf{Fc-P_2^+-C_{60}^- \rightarrow Fc-P_2-C_{60}}$	-1.30	$(160\ ps)^{-1}$	
$\mathbf{Fc^+-P_2-C_{60}^- \rightarrow Fc-P_2-C_{60}}$	-0.99	$(7100\ ps)^{-1}$	
$\mathbf{Fc-P_4^*-C_{60} \rightarrow Fc-P_4^+-C_{60}^-}$	-0.28	$(30\ ps)^{-1}$	65^b
$\mathbf{Fc-P_4^+-C_{60}^- \rightarrow Fc^+-P_4-C_{60}^-}$	-0.30	$(440\ ps)^{-1}$	26^c
$\mathbf{Fc-P_4^+-C_{60}^- \rightarrow Fc-P_4-C_{60}}$	-1.31	$(290\ ps)^{-1}$	
$\mathbf{Fc^+-P_4-C_{60}^- \rightarrow Fc-P_4-C_{60}}$	-1.01	$(7800\ ps)^{-1}$	

^{a} Driving forces were estimated from spectroscopic and electrochemical measurements (Supporting Information). ^{b} Quantum yield for the charge separated state ($\Phi_{CS} = k_{CS}/(\tau_{11}^{-1} + k_{CS} + k_Q)$). ^{c} Overall quantum yield for the fully charge separated state ($\Phi = \Phi_{CS} \times k_{CSh}/(k_{CR1} + k_{CSh})$).
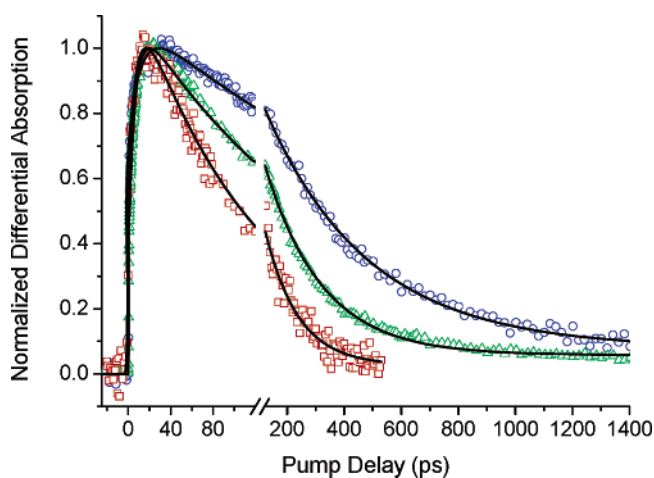
Figure 5. Normalized transient absorption decays and fitted curves for $\mathbf{Si-P_1-C_{60}}$ (excited at 450 nm, red squares), $\mathbf{Si-P_2-C_{60}}$ (excited at 490 nm, green triangles), and $\mathbf{Si-P_4-C_{60}}$ (excited at 490 nm, blue circles) probed at 1000 nm.

Once the initial charge separation has occurred, there are two possible pathways: First, a return to the ground state by charge recombination ($k_{CR1} = \tau_{22}^{-1}$) or, second, the formation of the fully charge separated state by hole transfer between the porphyrin oligomer and ferrocene (charge shift reaction, k_{CSh}). The lifetime of the first charge separated state in $\mathbf{Si-P_n-C_{60}}$ was measured from the decay of the porphyrin radical cation ($\mathbf{Si-P_n^+-Si}$) and fullerene radical anion ($\mathbf{C_{60}^-}$) to be between 130 and 300 ps (Table 1, Figure 5). When the rate constants, k_{CR1}, were tested with the Marcus equation, reasonable fits were found for the same electronic coupling as for the charge separation process ($V = 22.5\ cm^{-1}$). The reorganization energies found were, however, slightly larger at approximately $0.77-0.80$ eV.

These lifetimes provide the rate constant for charge recombination of the initial charge separated state, k_{CR1} (Table 2). In the charge shift reaction, the porphyrin oligomer radical cation decays and reforms the ground state while the fullerene radical anion remains unaffected. At the same time the ferrocene radical cation is formed, but its transient absorption is weak and overlaps with the stronger absorption of other species, which makes it difficult to use quantitatively. Thus, the rate constant for charge shift is estimated from the
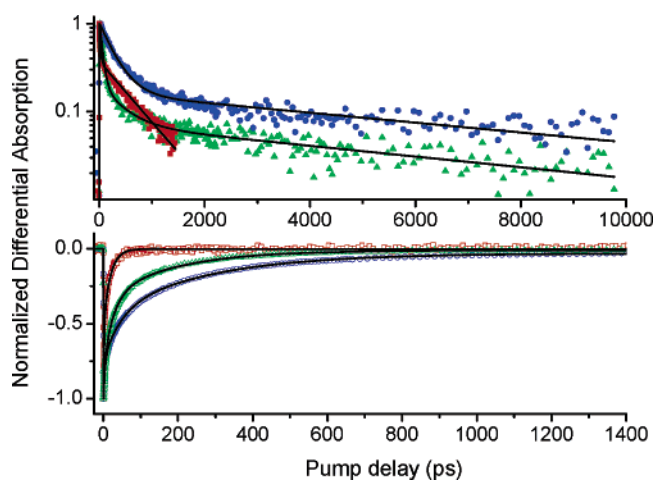
Figure 6. Transient absorption decays measured at 1000 nm (top), shown in logarithmic scale to emphasize the fact that they are single-exponential decays at long delay times. The bottom panel shows the ground-state recovery of the oligomers (660, 732, and 756 nm). $\mathbf{Fc-P_1-C_{60}}$ is shown by red squares; $\mathbf{Fc-P_2-C_{60}}$, by green triangles; and $\mathbf{Fc-P_4-C_{60}}$, by blue circles. Note the different scales of the abscissa in the two panels.

difference in decay rates of $\mathbf{P_n^+}$ in the triads (τ_{32}^{-1}) and $\mathbf{Si-P_n-C_{60}}$ dyads (eq 4).

$$k_{CSh} = 1/\tau_{32} - k_{CR1} \tag{4}$$

The introduction of the ferrocene secondary donor decreases the lifetime of the initial charge separated state to between 30 and 175 ps (Table 1). In all three triads significant amounts of the fully charge separated state are formed (overall quantum yields varying between 26% and 60%), and in the following the fate of this state will be discussed.

In the fully charge separated state, the distances between $\mathbf{C_{60}^-}$ and $\mathbf{Fc^+}$ are approximately 24, 38, and 65 Å in $\mathbf{Fc-P_1-C_{60}}$, $\mathbf{Fc-P_2-C_{60}}$, and $\mathbf{Fc-P_4-C_{60}}$, respectively, and the bridging porphyrin oligomers are in their electronic ground states. Figure 6 shows the transient absorption decays at wavelengths where, after an initial induction time, a clean single exponential $\mathbf{C_{60}^-}$ decay dominates the signal. The decay of the $\mathbf{Fc-P_1-C_{60}}$ system is evidently faster (0.64 ns) than those of both $\mathbf{Fc-P_2-C_{60}}$ and $\mathbf{Fc-P_4-C_{60}}$ (7.1 and 7.8 ns, respectively). In the lower panel of Figure 6, the porphyrin ground state recoveries of the corresponding systems are displayed. As expected from the model presented in Figure 1, the porphyrin ground state absorption recovers long before the charge separated states have decayed. The ground state recovery times agree well with the estimated decays of the porphyrin oligomers radical cations, further supporting the proposed model. The rate constants, k_{CR2}, for decay of the $\mathbf{Fc^+-P_n-C_{60}^-}$ ion pairs are all too fast for a significant contribution from a dynamic quenching process due to intermolecular electron transfer under the very dilute conditions of these experiments (concentration $\approx 10\ \mu M$).

Discussion of Electron-Transfer Rates. Compared to those of similar systems, the recombination rates, k_{CR2}, are remarkably fast,[5−7] which must be a consequence of the bridge-mediated electronic coupling. The distance dependence of k_{CR2} is also remarkable. If the logarithm of the rate constant for an electron-transfer reaction is plotted against the $Fc\cdots C_{60}$ distance, a straight line with slope $-\beta$ is expected from eq 1. In Figure 7, the logarithm of k_{CR2} is plotted against the fullerene−ferrocene distance and it is evident that the data do not describe a straight
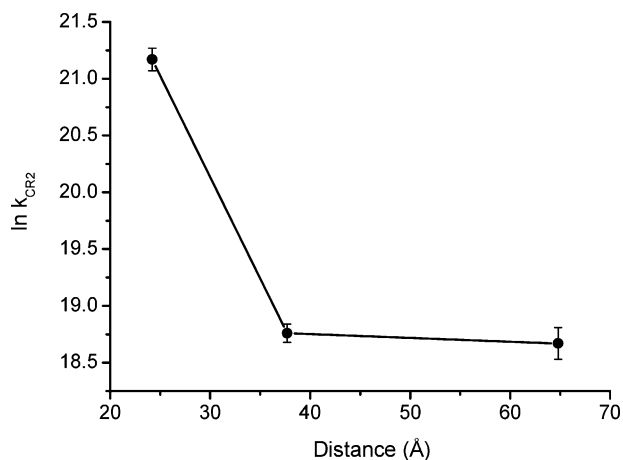
Figure 7. Semilogarithmic plot of the recombination rate versus the Fc···C_{60} distance in **Fc−P_1−C_{60}**, **Fc−P_2−C_{60}**, and **Fc−P_4−C_{60}**.

line. The slope of a line connecting the first two data points corresponds to $\beta = 0.18$ Å^{-1}, which is a value in the lower end of those typically found for conjugated bridge structures,[2−5] indicating a weak distance dependence, whereas connecting the second and third data points results in a line with practically no distance dependence ($\beta = 0.003$ Å^{-1}). Another way of quantifying the effectiveness of these bridges is to estimate the electronic coupling matrix element, V. The Marcus equation for nonadiabatic electron transfer, assuming a typical fullerene−ferrocene reorganization energy ($\lambda = 1.2$ eV),[6] gives $V = 3.3$, 0.92, and 0.85 cm^{-1} for recombination of **Fc$^+$−P_1−C_{60}^-**, **Fc$^+$−P_2−C_{60}^-**, and **Fc$^+$−P_4−C_{60}^-**, respectively. The coupling terms for the dimer and tetramer are similar to those reported in a 43 Å long phenylenethynylene bridge by Creager and co-workers (0.7 cm^{-1})[4a] and a 40 Å phenylenethynylene bridge reported by Wiberg et al. (1 cm^{-1})[4b] but much stronger than that reported for an analogous nonconjugated Fc-porphyrin−porphyrin−C_{60} system (5.6×10^{-5} cm^{-1}).[6] It is remarkable that the couplings through P_2 and P_4 are essentially the same.

Three mechanisms could contribute to charge recombination from the fully charge-separated states (**Fc$^+$−P_n−C_{60}^-**): (i) through-bond electron tunneling, (ii) electron or hole hopping, or (iii) recombination via a porphyrin oligomer triplet state.[19−21] Bridge-mediated through-bond electron transfer, typically described by the superexchange model,[19] is a mechanism by which bridge states are not populated during charge transfer. In the superexchange description, the rate for electron transfer decreases exponentially with donor−acceptor separation, and therefore this model does not adequately explain the data in Figure 7. Electron hopping is a mechanism by which bridge radical states are populated as kinetic intermediates, so that electron transfer takes place in a sequence of short steps.[22−26]

This requires a favorable energy difference between the states involved, and if they are resonant, or nearly so, a very weak distance dependence is generally found. In the present case repopulating the bridge would be endergonic (Figure 4) and thermal charge injection is unlikely to be a major contributor to the recombination process ($|\Delta G^\circ| \approx 10\ k_BT$). Moreover, the energy gaps are very similar for all three systems, and therefore recombination by electron hopping is probably not the explanation for the nonexponential behavior in Figure 7, as it would have a comparable effect in all three cases. The other possibility is that the charges recombine by forming a bridge triplet state. For the tetramer system the oligomer triplet state and the charge shifted state are almost isoenergetic (Figure 4), suggesting that recombination via a triplet state might be viable. This process would result in long-lived ground state bleaching, and this is observed to a small extent for the tetramer system, but the amount of bleaching does not increase on the time scale of the decay of the **Fc$^+$−P_n−C_{60}^-** state, and thus there is no evidence to indicate that the charge shifted state recombines to a bridge triplet state. It seems, therefore, that neither hopping nor triplet recombination makes significant contributions to the charge recombination process and that the reason for the nonexponential distance dependence lies elsewhere.

In the McConnell model, the bridge is treated as consisting of a number of pairwise interacting subunits, and between each unit there is a well-defined electronic coupling (ν). Moreover, it can be shown that the overall bridge electronic coupling is exponentially decreasing if ν is small compared to the tunneling barrier (approximately equal to $-\Delta G_{CSh}$ for the CR2 reaction). In the present case, there is strong conjugation between the porphyrin subunits and, further, a low tunneling barrier, and thus, the McConnell model might not be well-suited to describe the electron-transfer distance dependence of these systems.[27] From quantum mechanical time-dependent density functional theory calculations we have shown that the distance dependence of the donor−acceptor electronic coupling can be nonexponential for π-conjugated bridges that have strongly distance dependent state energies.[1] Possibly, each porphyrin oligomer bridge should instead be regarded as a single continuous energy barrier. The evolution of the excitation energies of the P_n oligomers is linear with the reciprocal oligomer length,[14] and thus the electronic structure of P_2 is more similar to that of P_4 than P_1. For example the third-order susceptibility, two-photon cross section, and excited-state polarizability all increase abruptly by more than an order of magnitude on going from P_1 to P_2 but increase only about 2-fold from P_2 to P_4.[28] The strong electronic coupling that gives rise to this nonlinear optical behavior also accounts for the pronounced difference in electron-transfer properties between the monomer and the oligomers. The observation that **Fc$^+$−P_2−C_{60}^-** and **Fc$^+$−P_4−C_{60}^-** give essentially the same charge recombination rate, despite their very different lengths, implies that the tunneling barrier in these systems is mainly associated with the junctions to the electron donor and acceptor components and that there is very little

(19) Ishimura, K.; Hada, M.; Nakatsuji, H. *J. Chem. Phys.* **2002**, *117*, 6533−6537. Rohmer, M.-M.; Veillard, A.; Wood, M. H. *Chem. Phys. Lett.* **1974**, *29*, 466−468. Armstrong, A. T.; Smith, F.; Elder, E.; McGlynn, S. P. *J. Chem. Phys.* **1967**, *46*, 4321−4328.
(20) McConnell, H. *J. Chem. Phys.* **1961**, *35*, 508−515.
(21) Harriman, A.; Khatyr, A.; Ziessel, R.; Benniston, A. C. *Angew. Chem., Int. Ed.* **2000**, *39*, 4287−4290. Harriman, A.; Rostron, S. A.; Khatyr, A.; Ziessel, R. *Faraday Discuss.* **2006**, 377−391.
(22) Davis, W. B.; Svec, W. A.; Ratner, M. A.; Wasielewski, M. R. *Nature* **1998**, *396*, 60−63.
(23) Winters, M. U.; Pettersson, K.; Martensson, J.; Albinsson, B. *Chem.−Eur. J.* **2005**, *11*, 562−573.
(24) Lambert, C.; Nöll, G.; Schelter, J. *Nat. Mater.* **2002**, *1*, 69−73.
(25) Weiss, E. A.; Ahrens, M. J.; Sinks, L. E.; Gusev, A. V.; Ratner, M. A.; Wasielewski, M. R. *J. Am. Chem. Soc.* **2004**, *126*, 5577−5584.

(26) Weiss, E. A.; Tauber, M. J.; Kelley, R. F.; Ahrens, M. J.; Ratner, M. A.; Wasielewski, M. R. *J. Am. Chem. Soc.* **2005**, *127*, 11842−11850.
(27) Reimers, J. R.; Hush, N. S. *Nanotechnology* **1996**, *7*, 417−423.
(28) Drobizhev, M.; Stepanenko, Y.; Rebane, A.; Wilson, C. J.; Screen, T. E. O.; Anderson, H. L. *J. Am. Chem. Soc.* **2006**, *128*, 12432−12433. Thorne, J. R. G.; Kuebler, S. M.; Denning, R. G.; Blake, I. M.; Taylor, P. N.; Anderson, H. L. *Chem. Phys.* **1999**, *248*, 181−193. Piet, J. J.; Taylor, P. N.; Wegewijs, B. R.; Anderson, H. L.; Osuka, A.; Warman, J. M. *J. Phys. Chem. B*, **2001**, *105*, 97−104.

barrier to tunneling through the conjugated porphyrin oligomer. It further implies that it is insufficient to condense the distance dependence into a single parameter, such as β.

Conclusions

The rate of charge recombination in $\mathbf{Fc^+ - P_n - C_{60}^-}$ is remarkably fast and exhibits very weak distance dependence, particularly when comparing the systems with $n = 2$ and $n = 4$. This long-range charge recombination process appears to take place via electron tunneling rather than via hopping or triplet recombination. Future work will be aimed at further clarifying the charge recombination mechanism by also investigating the temperature dependence of this process. The expected difference in activation energy between electron tunneling and hopping should make it possible to distinguish these mechanisms from the temperature dependence of the recombination rates, k_{CR2}. This requires, however, that the electronic couplings of the systems do not vary significantly with temperature. The description of the charge recombination is complicated by the fact that it is mediated by the oligomers in the ground state, in which they are essentially free to rotate around the butadiyne axis. The conformational distribution of the oligomers is broad at room temperature but becomes more biased toward, on average, more planar conformations at lower temperature. This augments the electronic coupling, which is a strong function of the porphyrin–porphyrin dihedral angle, and it is therefore not clear whether a temperature study will provide definite discrimination between hopping and tunneling. A parallel study addresses the question of conformational heterogeneity and considers the conformational dependence of both charge separation and charge recombination.[29] The complexity of this question demands a detailed study that is beyond the scope of the present paper. Although the exact mechanism of electron transfer in these systems remains to be elucidated, the observation that the porphyrin tetramer mediates fast long-range charge transfer, over 65 Å, is significant for the application of these structures as molecular wires. A key question for future research is whether the very small distance dependence in the electron-transfer rates in $\mathbf{P_2}$ and $\mathbf{P_4}$ extends to longer oligomers such as $\mathbf{P_8}$ and $\mathbf{P_{16}}$, giving access to effective molecular wires with lengths in excess of 10 nm.

Supporting Information Available: Ground state absorption spectra, spectroelectrochemistry, redox potentials, geometry calculations, calculation of state energies, time-resolved fluorescence and transient absorption, synthetic procedures, and characterization data. This material is available free of charge via the Internet at http://pubs.acs.org.

JA067447D

(29) Winters, M. U.; Kärnbratt, J.; Blades, H. E.; Wilson, C. J.; Frampton, M. J.; Anderson, H. L.; Albinsson, B. Manuscript in preparation.